Peer-reviewed version available at *Proteomes* **2019**, *7*, 5; doi:10.3390/proteomes7010005

Research Article

Sex-Specific Proteomics Changes Induced by Genetic Deletion of the Fibroblast Growth Factor 14 (FGF14) Regulator of Neuronal Ion Channels

Mark L Sowers[1,2,5], Jessica Di Re [2,3,5], Paul A Wadsworth[1,2,4], Alexander S Shavkunov[2], Cheryl Lichti[2], Kangling Zhang[2], and Fernanda Laezza [2,*]

[1] UTMB MD/PhD Combined Degree Program, University of Texas Medical Branch, Galveston, TX, USA; mlsowers@utmb.edu

[2] Department of Pharmacology and Toxicology, University of Texas Medical Branch, Galveston, TX, USA; asshavku@utmb.edu (A.S.), clichti@wustl.edu (C.L.) kazhang@utmb.edu (K.Z.), felaezza@utmb.edu (F.L.)

[3] Neuroscience Graduate Program, University of Texas Medical Branch, Galveston, TX, USA; jedire@utmb.edu (J.D.)

[4] Biochemistry and Molecular Biology Graduate Program, University of Texas Medical Branch, Galveston, TX, USA pawadswo@utmb.edu (P.W.)

[5] These authors contributed equally

* Correspondence: felaezza@utmb.edu; Tel.: +1-409-772-9672

Abstract: Fibroblast growth factor 14 (FGF14) is a member of the intracellular FGFs, a group of proteins with roles in neuronal ion channel regulation and synaptic transmission. We have previously demonstrated that a male Fgf14-/- mouse model recapitulates salient endophenotypes of synaptic dysfunction and behaviors associated with schizophrenia (SZ). As the underlying etiology of SZ and its sex-specific onset remain elusive, the Fgf14-/- model provides a valuable tool to interrogate pathways that might be related to the disease mechanism. Here, we performed label free quantitative proteomics and bioinformatics to identify enriched pathways at the proteome level in the male and female hippocampi from Fgf14+/+ and Fgf14-/- mice. We discovered that many differentially expressed proteins in Fgf14-/- animals are associated with SZ. In addition, measured changes in the proteome and signaling pathways were predominantly sex-specific with the male Fgf14-/- being distinctly enriched for pathways associated with neuropsychiatric disorders and addiction and the female exhibiting modest changes. In the male Fgf14-/- mouse the major protein changes that could in part explain the previously described neurotransmission and behavioral phenotype of this model were loss of ALDH1A1 and PRKAR2B. ALDH1A1 has been shown to mediate an alternative pathway for GABA synthesis, while PRKAR2B is essential for dopamine 2 receptor signaling, which is the basis of current antipsychotics. Collectively, our results provide new insights in the role of FGF14 and support the use of the Fgf14-/- mouse as a useful preclinical model of SZ for generating hypothesis on the disease mechanism, sex-specific manifestation and therapy.

Keywords: Mass Spectroscopy, Bioinformatics, FGF14, Voltage Gated Channels, Schizophrenia, Alzheimer's Disease, Sex-Specific Differences, Synaptic Plasticity, Cognitive Impairment, Excitatory/Inhibitory Tone

1. Introduction

Originally identified as the genetic locus of missense mutations leading to spinocerebellar ataxia type 27 [1–7], FGF14 is an emerging risk factor for neuropsychiatric disorders [8]. Unlike canonical secreted FGFs, which act through activation of FGF receptor signaling, FGF14 is retained intracellularly where it has been shown to regulate ion channel function [9–13]. Extensive evidence indicates that FGF14 within neurons binds directly to and regulates the voltage-gated sodium (Nav) channel targeting at the axonal initial segment (AIS) and biophysical properties [9–13,18–21]. Other

reported functions of FGF14 suggest a much more complex role of this protein within the brain including regulation of presynaptic glutamate and gamma-amino-butyric acid (GABA) release and calcium signaling [18–21]. Studies focusing on signaling pathways have demonstrated that FGF14 is also a hub for regulatory kinases [11,22], including glycogen synthase kinase 3 [15], an enzyme which has been linked to depression, bipolar disorder and schizophrenia (SZ) [8,23–25].

Given the variety of key cellular functions associated with FGF14, it is not surprising that deletion of the gene results into disrupted function and behavior associated with complex brain disorders. Recent studies have shown that male mice lacking *Fgf14* (*Fgf14*-/-) recapitulate key features of endophenotypes of SZ. Namely, male *Fgf14*-/- mice are presented with loss of parvalbumin positive GABAergic interneurons in the hippocampus, disrupted gamma frequency and reduced working memory, hallmarks of cognitive impairment in SZ in animal models and post-mortem studies [21,26]. Concomitant changes in these mice are found at glutamate synapses with reduced presynaptic release and long-term potentiation [20,27] which could all be part of a common underlying pathology of SZ and other neurodevelopmental disorders [28]. Additional evidence of disease endophenotypes is brought by studies reporting disrupted adult neurogenesis in the dentate gyrus (DG) of *Fgf14*-/- mice that is consistent with an immature dentate gyrus [21,29] and is another hallmark of SZ and other neuropsychiatric disorders [30].

In addition to reduced working memory, male *Fgf14*-/- mice exhibit behavioral deficits that align with disrupted dopamine signaling, including altered aggressive and reproductive behavior, and blunt response to cocaine and methamphetamine [26,31].

Taken together, these finding indicate that the male *Fgf14*-/- mouse recapitulates endophenotypes of SZ, linked to changes in GABA and glutamate synaptic signaling, leading to perturbations of the excitatory/inhibitory (E/I) tone of the brain [32–36], impaired neurogenesis in the DG and disruption of dopamine signaling, that are all functional nodes in the pathophysiology of SZ.

Though many lines of evidence converge to suggest that male *Fgf14*-/- mice are a useful animal model for the study of SZ and other neuropsychiatric disorders, little is known about how these complex phenotypes develop and whether sex-specific differences exist in female *Fgf14*-/- animals.

We have chosen to investigate this potentially useful animal model using label free proteomics to gain further insights into the etiology of SZ and related disorders as well as evaluation of similarity between this animal model and patients afflicted with SZ. Thus, we isolated hippocampi from male and female *Fgf14*+/+ and *Fgf14*-/- mice and performed label free proteomic mass spectrometry and a variety of bioinformatics approaches to determine molecular pathways disrupted in this model, as well as elucidate sex-specific interactions with FGF14. These experiments will aid in the generation of new hypotheses about neuropsychiatric diseases, as well as possibly elucidate several gender-specific differences in the etiology of SZ, such as age of diagnosis, symptom clustering, premorbid function, treatment response and prognosis [37–41].

2. Materials and Methods

2.1 Hippocampal tissue preparation

Both hippocampi were dissected from each mouse brain, and samples from the animals belonging to the same experimental group were combined together for protein extraction (n=3) and run three separate times for technical replicates. Tissue was homogenized in RIPA buffer (Thermo Fisher Scientific, Rockford, IL, 25 mM TrisHCl pH 7.6, 150 mM NaCl, 1% NP-40, 1% sodium deoxycholate, 0.1% SDS) containing Halt protease and phosphatase EDTA-free inhibitor cocktail (Thermo Fisher Scientific, Rockford, IL) and 1 mM phenylmethylsulfonyl fluoride. Mechanical homogenization was performed using Polytron™ PT 10/35 GT Homogenizer (Kinematica, Bohemia, NY), 20 s x 3 pulses, 10000 rpm. After homogenization, Pierce universal nuclease (Thermo Fisher Scientific, Rockford, IL)

was added to the samples (25 units per 1 ml of tissue lysate) and they were incubated on ice for 30 min. Protein concentration was determined by BCA Protein Assay Kit (Pierce), and an aliquot of each sample containing 100 µg total protein was reduced and alkylated. Five µL of 200 mM tris (2-carboxyethyl) phosphine (TCEP) buffered with 50 mM triethylammonium bicarbonate (TEAB) was added to each sample (final TCEP concentration 10 mM) and incubated at 55 °C for 1 h. Five µL of 375 mM iodoacetamide (buffered with 50 mM TEAB) was added and incubated in the dark for 30 min. Proteins were precipitated in four volumes (440 µL) of ice cold acetone overnight at −20 °C. Samples were centrifuged at 10 000g for 30 min (4 °C), after which the supernatants were removed and discarded. Protein pellets were de-lipidated according to Mastro, 1999 by incubation in 1 ml of ice-cold tri-n-butylphosphate/acetone/methanol (1:12:1 by volume), followed by centrifugation at 2800 g for 15 min, 4◎C, and sequential incubations in ice-cold tri-n-butylphosphate, acetone and methanol, 15 min each. Pellets were air-dried and resuspended in 12.5 µL of 8 M urea. Trypsin (4 µg in 87.5 µL of TEAB buffer) was added, and the samples were incubated for 24 h at 37 °C. Final sample clean-up and removal of urea was performed using Mark C18 Sep-Pak® Vac 1cc cartriges (Waters) attached to a vacuum manifold. Cartridges were pre-equilibrated with 3 × 1 ml acetonitrile and washed with 3 × 1 ml of 0.25% trifluoroacetic acid (flow rate ~ 2 ml/min); digested samples were loaded on the cartridges after adding trifluoroacetic acid to 1% final concentration, washed with 4 × 1 ml of 0.25% trifluoroacetic acid, eluted in 1 ml of 80% acetonitrile /0.1% formic acid, and dried in the CentriVamp Concentrator (Labconco, Kansas City, Missouri).

Protocol Number: 0904029C

Protocol Title: The Physiological Role of FGF-14 in the Brain of Rodents

2.*2 Mass Spectrometry and chromatography*

Chromatographic separation and mass spectrometric analysis was performed with a nano-LC chromatography system (Easy-nLC 1000, Thermo Scientific) coupled online to a hybrid linear ion trap-Orbitrap mass spectrometer (Orbitrap Elite, Thermo Scientific) through a Nano-Flex II nanospray ion source (Thermo Scientific). Mobile phases were 0.1% formic acid in water (A) and 0.1% formic acid in acetonitrile (ACN, B). After equilibrating the column in 95% solvent A and 5% solvent B, the samples (5 µL in 5% v/v ACN/0.1% (v/v) formic acid in water, corresponding to 1 µg of tissue protein digest) were injected onto a trap column (C18, 100 µm ID × 2 cm) and subsequently eluted (250 nL/min) by gradient elution onto a C18 column (10 cm × 75 µm ID, 15 µm tip, ProteoPep II, 5 µm, 300 Å, New Objective). The gradient was as follows: isocratic flow at 5% Solvent B for 5 minutes, 5% to 35% Solvent B for 89 minutes, and 35% to 95% Buffer B for 16 minutes followed by isocratic flow at 95% Buffer B for 10 minutes.

All LC–MS/MS data were acquired using XCalibur, version 2.7 SP1 (Thermo Fisher Scientific). The survey scans (m/z 350–1650) (MS) were acquired in the Orbitrap at 60 000 resolution (at m/z = 400) in profile mode, followed by top 5 higher energy collisional dissociation (HCD) fragmentation centroid MS/MS spectra, acquired at 15K resolution in data-dependent analyses (DDA) mode. The automatic gain control targets for the Orbitrap were 1 × 106 for the MS scans and 5 × 104 for MS/MS scans. The maximum injection times for the MS1 and MS/MS scans in the Orbitrap were both 500 ms. For MS/MS acquisition, the following settings were used: parent threshold = 10 000; isolation width = 4.0 Da; normalized collision energy = 30%; and activation time = 10 ms. Monoisotopic precursor selection, charge-state screening, and charge-state rejection were enabled, with rejection of singly charged and unassigned charge states. Dynamic exclusion was used to remove selected precursor ions (∓10 ppm) for 90 s after MS/MS acquisition. A repeat count of 1 and a maximum exclusion list size of 500 were used. The following ion source parameters were used: capillary temperature 275 °C, source voltage 2.1 kV, source current 100 uA, and S-lens RF level 40%. Each sample was run in triplicate, and the order of runs was block-randomized.

2.3 Quantification of peptides and proteins

Maxquant version 1.6.1.0 was used to process raw files [43,44]. Default setting were used unless otherwise specified. Briefly, peptide-spectrum-match and protein FDR were set to 1% and a minimum of 1 unique peptide for identification. Fixed modifications were set to carbamidomethyl for cysteine and variable modifications to methionine oxidation and N-terminal acetylation. Match between runs was enabled with default match time window of 0.7 min and alignment window of 20 minutes. The mouse Uniprot reference proteome was downloaded on 9/18/2018, last updated 7/28/2018, with canonical and isoform sequences. For label free quantification (LFQ) MS2 was required, a minimum of 1 peptide was required for quantification across samples including both razor and unique peptides.

2.4 Statistical Analysis

Statistical analysis was performed in the Perseus 1.6.0.7 [45]. LFQ intensity values were log2 transformed to make the data normally distributed. Proteins identified by site, reverse, and potential contaminants were filtered prior to analysis. Proteins with missing values in any sample including replicates were filtered. Differentially expressed proteins were determined using a moderated t test statistic with FDR-controlled at 5% and s0 parameter set to 0.1. FDR was calculated using a permutation-based method with 250 randomizations between groups.

3. Results

In order to efficiently detect specific changes in the cellular proteome, it is important to limit the biological complexity of the subject of study. Whole brain proteome analysis is likely to miss or downplay prominent changes of protein expression in particular brain regions, proteomic analysis of isolated brain structures being significantly more sensitive. Previous studies, including our own work, have been largely focusing on the important physiological role of FGF14 in the hippocampus, the part of the limbic system which is critically involved in the cognitive processes, and also one of the primary sites of FGF14 expression in the brain [13,20,31]. FGF14 knockout causes pronounced changes in synaptic transmission [20,21] and cellular composition [21,29] of the hippocampus which correlate with changes in electrophysiology as well as behavioral deficits [20,27,31]. All of this information gives an important framework for meaningful interpretation of the proteomic data. Given the documented role of hippocampal pathology in cognitive impairment in SZ [49–52] it would be logical to hypothesize that these gross changes play a critical part in the development of SZ-related endophenotypes in the *Fgf14-/-* mice. An additional advantage is that hippocampus can be readily isolated from the adjacent brain structures, which makes sample preparation more robust and reproducible. The workflow of our study is presented in **Figure 1**.

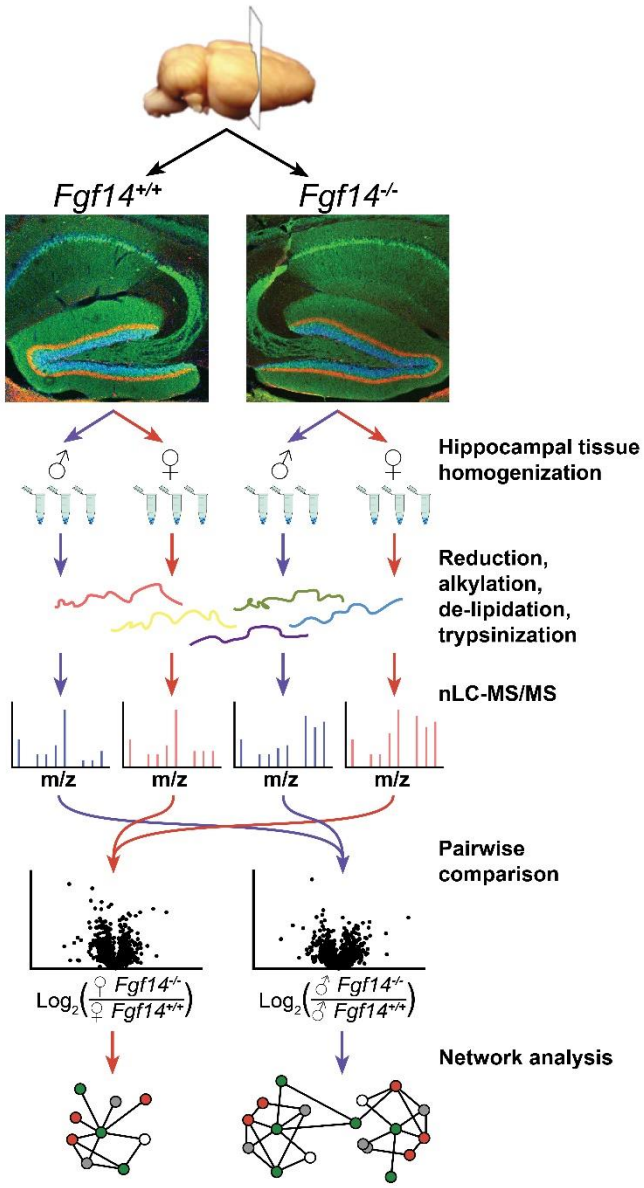

Figure 1. Figure 1. Overview of label free proteomics workflow and analysis (Figure 1. Overview of label free proteomics workflow and analysis [46-48]. Workflow outlining experimental procedures and nLC-MS/MS data acquisition for analysis of hippocampal brain tissue from male and female fgf14¬+/+ ¬and fgf14¬-/- mice as detailed in the text. Representative confocal images of triple staining of the entire hippocampus from fgf14¬+/+ ¬(left) and fgf14¬-/- (right) mice representing calbindin (green), calretinin (red), and Topro-3 nuclear staining (blue) at low magnification of the Dentate Gyrus (DG).

While having many advantages, mostly regarding ease of use, label free proteomics is important to standardize chromatography conditions and assess reproducibility and overall data quality. As shown in **Figure 2** the various samples and their technical replicates are shown to be highly reproducible after appropriate filtering (see methods). Furthermore, Maxquant quantifies protein intensity using MS2 spectra. However, if MS2 spectra for a peptide is missing in one run, due to the stochastic nature of data-dependent-acquisition, Maxquant has the match between run feature which allows for quantification by imputing the estimated MS2 intensity as long as there is an

appropriate MS1 peak for the corresponding peptide [43,44]. In our case this allowed recovery of ~16% of proteins to be quantified and overall ~2300 proteins quantified per run prior to filtering.

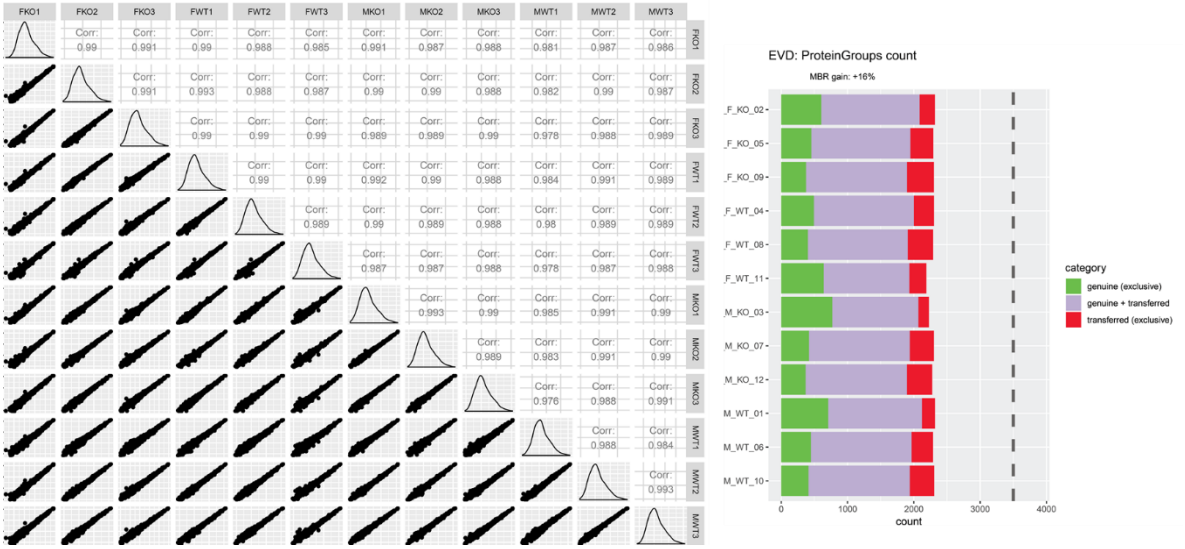

Figure 2. Quality control of label free quantitative proteomics. The Scatter matrix shows the pairwise Pearson correlations between animal groups and their technical replicates, histograms of log2(LFQ intensity) distributions, and their respective scatter plots. On the right is a quality control figure showing ~2300 proteins identified in each sample after applying match-between-runs (MBR) in Maxquant. The majority of proteins were identified across all samples by MS2 (purple), with a subset only identified in a given run (green), and an additional gain of 16% of identified proteins after retention time and m/z alignment of MS1 peaks (red). Quality control figure prepared using PTXQC [53].

3.1 Differentially expressed proteins in fgf14-/- mice and their implications

After log transformming and filtering we analyzed ~1500 proteins whose distribution was approximately normal across all samples. We then compared male and female *Fgf14-/-* to their respective wildtypes using statistical analysis of microarrays, a moderated t-test statistic (**Figure 3**, Table S1). In the female *Fgf14-/-* mice we found *Snap25* and *Mtatp6* upregulated. SNAP25 is part of the SNARE complex that mediates neurotransmitter-vesicle fusion and controls receptor trafficking at post-synaptic sites of glutamatergic and GABAergic synapses [54]. It is unclear how genetic deletion of FGF14 causes a change in SNAP25 expression, but direct interaction bewteen the two molecules is a hypothesis, supported by previous proteomic studies showing FGF14 immunoprecipitation with SNAP25 [10]. Thus, genetic deletion of FGF14 could lead to SNAP25 loss of function, which in animal models is considered a mechansim leading to endophenotypes of SZ [55].

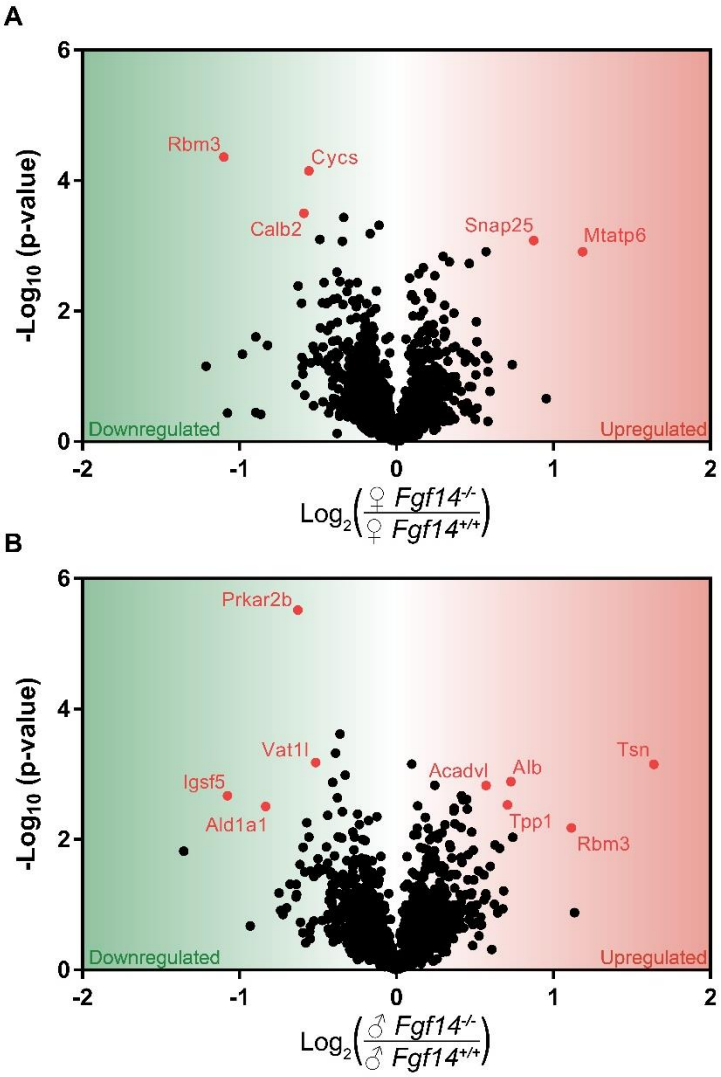

Figure 3. Volcano plot of mass spectrometry results showing proteins that are significantly upregulated in sex by genotype conditions. (**a**) shows the proteins significantly upregulated in female *Fgf14*+/+ compared to *Fgf14*-/- mice. (**b**) shows the proteins significantly upregulated in male *Fgf14*+/+ compared to *Fgf14*-/- mice. Y-axis represents negative log10 fold change and proteins with a positive Log2 fold change (FC) are upregulated and negative values represent downregulated proteins in the *Fgf14*-/- mice, respectively.

Another protein found dysregulated is MTATP6, also known as ATP synthase or Complex V, which has also been implicated in SZ both as a site of polymorphisms and as well as with reduced mRNA [56,57]. Furthermore, the soluble component of Cytochrome C (*Cycs*) was downregulated. CYCS is an essential component of Oxidative phosphorylation which is a major source of energy, particularly in neurons and mitochondrial dysfunction is believed to be one of the potential risk factors of SZ [56]. Finally, Calretinin (*Calb2*), a calcium buffering protein predominantly expressed in a subtype of hippocampal interneurons [58] was downregulated, which might be causative of or correlated with loss of calretinin positive interneurons. Although, CALB2 positive interneurons have not been directly linked to SZ [59], reduction of this protein could limit the intracellular calcium bufferring capacity of subtypes of interneurons reducing the overall GABAergic tone in the hippocampal circuit.

To our surprise, SNAP25 and MTATP6 were upregulated in the female mice but were not statistically significant in the male mice after multiple hypothesis test correction. This suggests that

Preprints (www.preprints.org) | NOT PEER-REVIEWED | Posted: 19 November 2018 doi:10.20944/preprints201811.0463.v1

Peer-reviewed version available at Proteomes 2019, 7, 5; doi:10.3390/proteomes7010005

the female *Fgf14-/-* mice may somehow be more resistant to the potential changes in mitochondrial function and GABA-ergic signalling suggested by changes in *Calb2* and *Cycs*.

While the differentially expressed proteins were almost entirely different between female Fgf14-/- and male Fgf14-/- compared to their respective Fgf14+/+ controls, there was one protein that they shared, Rbm3. RBM3 is a cold inducible protein that is believed to be protective against neurodegeneration and that mediates structural plasticity 59. As it is differentially regulated in the male and female Fgf14-/- mice, the upregulated in the male Fgf14-/- might be part of a stress response important in neurodegeneration.

3.2 Differentially expressed proteins highly associated with Schizophrenia and or Autism

Based on our literature search we had found a great deal of evidence that the differentially expressed proteins were associated with SZ as anticipated. Interestingly, we discovered that in an analysis of various GWAS studies, all of our proteins, with exception of Mtatp6, were identified to be statistically associated with either Autism and or SZ using the MAGMA tool that controls for various confounders to determine p-values for each protein coding gene [60,61] (**Figure 4**, Table S2). MTATP6 was likely missing due to its mitochondrial origin.

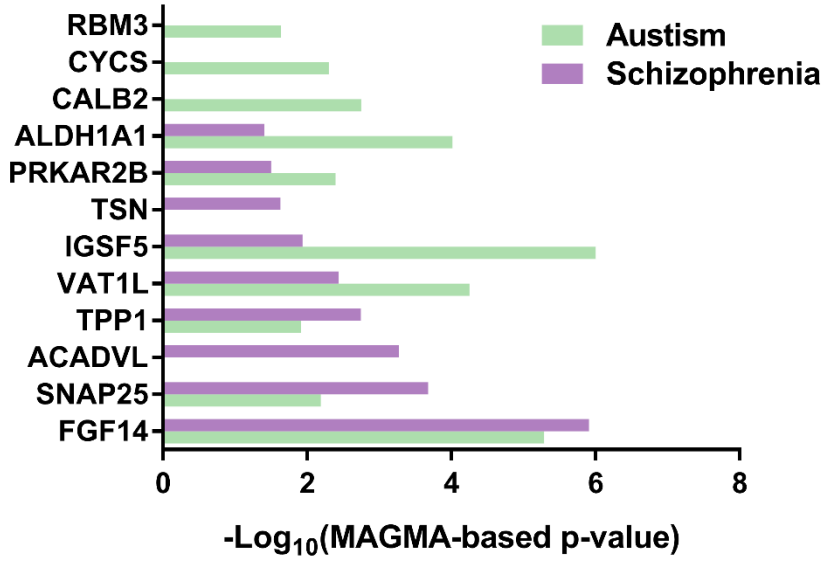

Figure 4. Differentially expressed proteins in *fgf14-/-* mice. Proteins with changes expression in *fgf14-/-* are associated with Autism and Schizophrenia based on analysis of genome-wide-association-study (GWAS) data from Seyfried et al. using the MAGMA tool [61].

3.2 ALDH1A1 and SNAP25 central roles in pathophysiology of fgf14-/- mice

Experimental protein-protein interaction networks were constructed with the differentially expressed proteins for males and females, seperately, using OmicsNet which identifies known interactors [62] (**Figure 5**). Interactions were based only on the high-confidence STRING interactions with experimental evidence. The networks were than imported into cytoscape for visual purposes. 3-Dimensional predicted Protein-Protein interaction networks were constructed with the differentially expressed proteins for males and females seperately (**Figure 5).** The network construction did not generate any connections to other significant proteins other than *Snap25* and *Aldh1a1* for females and males, respectively. Although protein-protein interaction data is far from complete this suggests that Snap25 and Aldh1a1 may be key players in the pathogenesis observed in the *Fgf14-/-* mice and perhaps SZ.

Preprints (www.preprints.org) | NOT PEER-REVIEWED | Posted: 19 November 2018 doi:10.20944/preprints201811.0463.v1

Peer-reviewed version available at Proteomes 2019, 7, 5; doi:10.3390/proteomes7010005

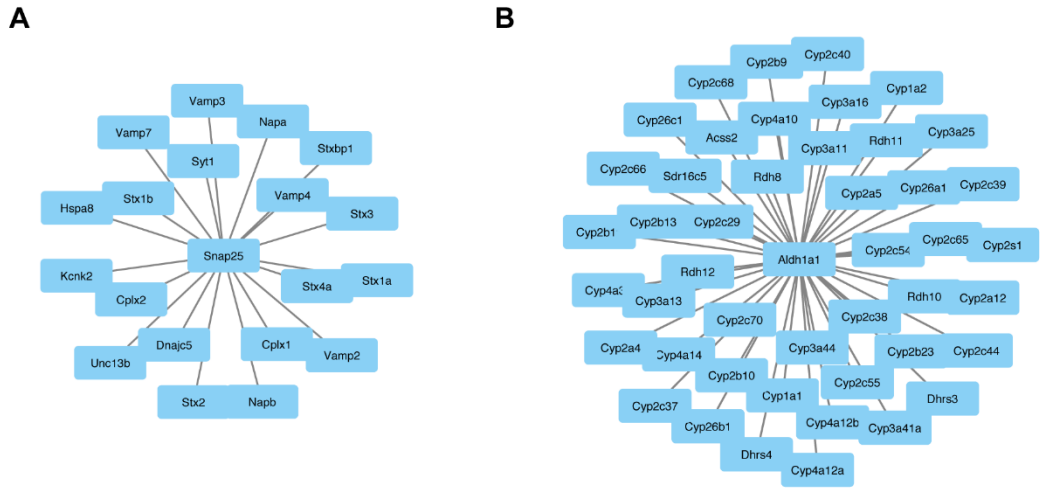

Figure 5. Central node proteins networks. Omicsnet was used to generate protein-protein networks with differentially expressed proteins and known experimental interactors. The networks created based on input gene names are shown for both the male and female *fgf14-/-* mice. In the center are the input genes and connected genes are known interactors. This analysis identified *Snap25* (**a**) and *Aldh1a1* (**b**) in female and male *fgf14-/-* mice, respectively.

3.3 Hierarchical clustering reveals subtype specific clusters

We performed hierarchical clustering using Euclidean distances in Perseus, displayed as a heatmap (**Figure 6**). Our analysis demonstrated four protein clusters that appear to be upregulated in each of the respective animals. We submitted these group specific clusters to the STRING protein-protein network database using only the highest confidence interactions based on all data types and identified positively enriched pathways for each animal specific protein cluster (**Figure 7**, Table S3).

Of particular note is that the enriched pathways in the male *Fgf14-/-*, which includes alcoholism, drug addiction, and related pathologies. These pathways may explain the endophenotype of the male *Fgf14-/-* mouse. Furthermore, all animal groups had enriched terms related to vesicle, membrane-bound vesicle, or vesicle-mediated transport likely indicating their important roles in the mouse hippocampus. This also suggests that both sex and presence of FGF14 may affect different aspects of neurotransmission given that these terms are positively enriched in all protein clusters.

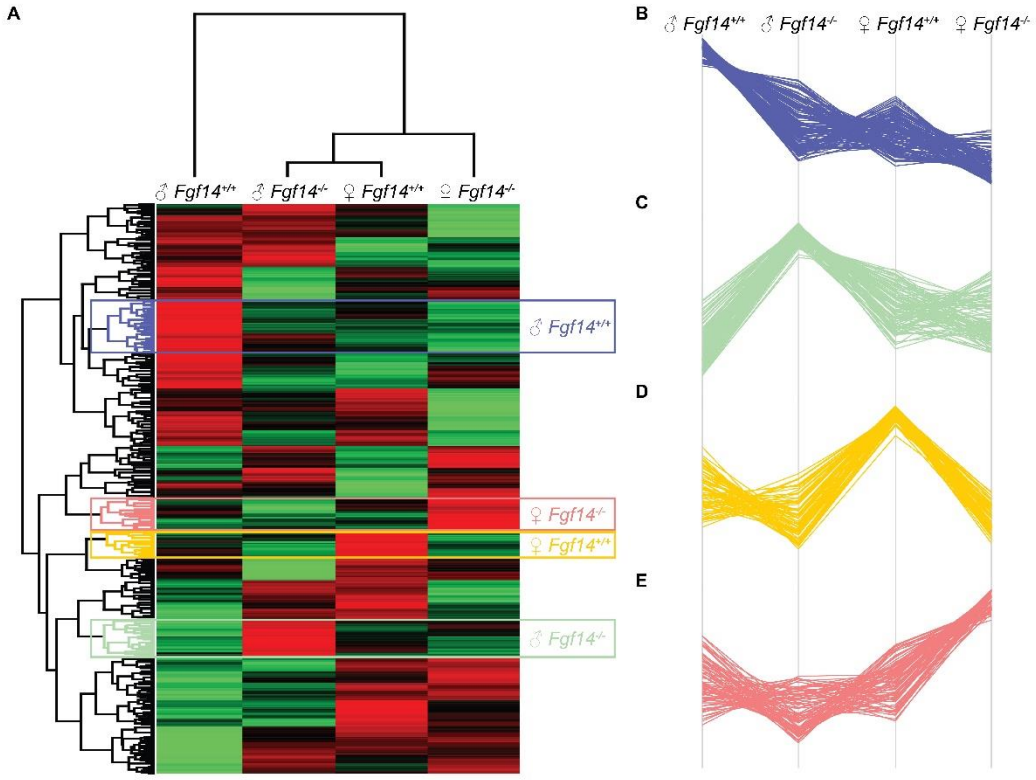

Figure 6. Hierarchical clustering, heatmap and cluster analysis of differentially expressed proteins. (**a**) Heatmap of differentially expressed proteins in male and female *fgf14*+/+ and *fgf14*-/- mice. LFQ intensities were averaged for technical replicates and averages across animal groups were Z-scored prior to Euclidean distance based hierarchical clustering with Perseus (**b-e**). Protein clusters specific to each animal group, male *fgf14*+/+, female *fgf14*-/-, female *fgf14*+/+ and male *fgf14*-/-, respectively.

3.4 Group specific cluster pathway enrichment shows addiction and various neurotransmitter gene ontology terms and KEGG pathways enriched in the male fgf14-/-.

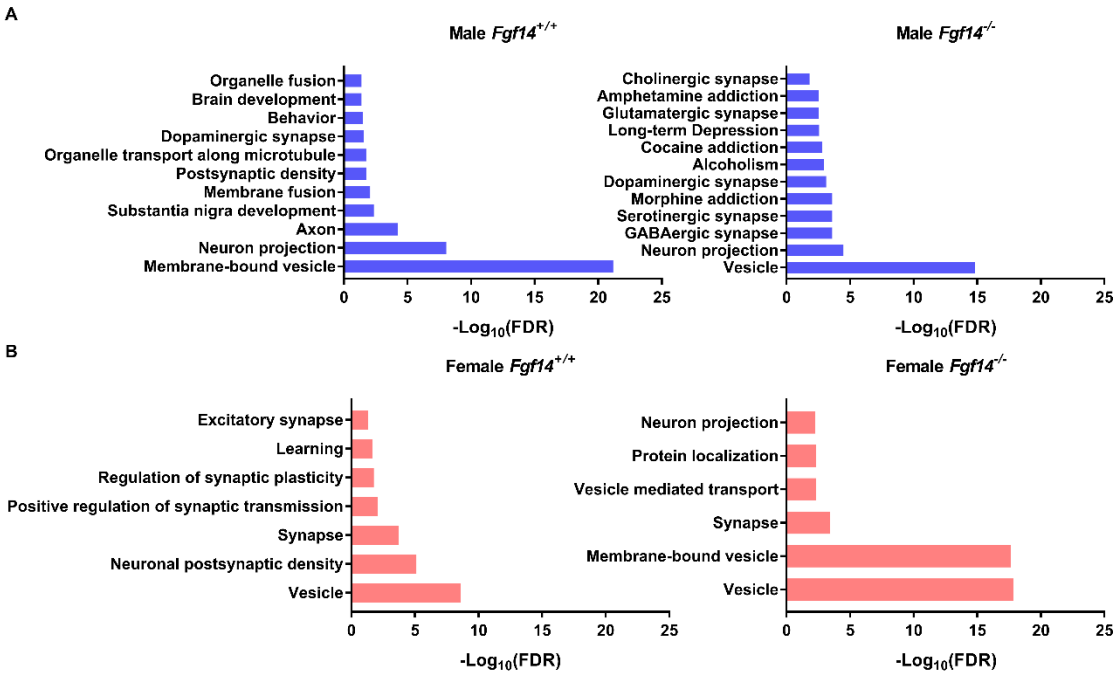

Figure 7. Protein-protein interaction and pathway enrichment for animal specific clusters. (**a**) Enriched pathways and their adjusted P-values (FDR) were obtained from the STRING database after inputting of cluster specific gene names. Male *fgf14*$^{-/-}$ display broad neurotransmitter based synaptic activation, drug addiction, and alcoholism. This was unique to the male *fgf14*$^{-/-}$ specific cluster. (**b**) Corresponding analysis for females.

4. Discussion

Using a label free proteomic approach and bioinformatics, we analyzed sex-specific differences in the hippocampi of *fgf14-/-* mice. Much research has shown that male *fgf14-/-* mice are presented with cognitive deficits and changes in neuronal function that mimic endophenotypes of SZ and other neuropsychiatric disorders [21,29], however the results presented in this study provide a biological context as to which specific pathways might be disrupted. Importantly, we found that many of the proteins that were differentially expressed in the male *fgf14-/-* mice have previously been linked to neuropsychiatric disorders with cognitive impairment, such as SZ and Autism (**Figure 4**). In fact, network analysis of proteomic data from brains of AD patients has shown that synaptic transmission, synaptic membrane, and mitochondrion are all pathways that are disrupted [60. Perhaps this indicates a general mechanism for cognitive impairment that may be related to SZ, Autism, and even cognitive aspects of Alzheimer's Disease (AD).

Importantly, many of the proteins with significantly changed expression in the male *fgf14-/-* mice, including ALDH1A1, PRKAR2B, and VAT1L, have previously been linked to SZ and other neuropsychiatric disorders with a domain of cognitive symptoms (**Figure 3**) [63–66]. These results also further support the role of FGF14 in synaptic signaling [18,21]. It has already been shown that *fgf14-/-* male mice are presented with changes in GABAergic signaling in the hippocampus [18,21], but our results suggest that FGF14 may regulate the composition of GABAergic synapses both presynaptically and postsynaptically through SNAP25 (**Figure 3,4**) and receptor trafficking (**Figure 7**).

Alterations in the dopaminergic signaling of male *fgf14-/-* mice may be due to changes in ALDH1A. ALDH1A is not only an important enzyme for the breakdown of alcohol, but also defines a subpopulation of DA neurons in the rodent and human Substantia Nigra pars compacta which are sensitive to α-synuclein cytotoxity [64]. As shown in Liu et al., deletion of ALDH1A1 exacerbates

dopaminergic neurodegeneration in mouse model of Parkinson's Disease. This effect may be mediated through changes in the E/I tone of the brain, as retinoic acid, which is synthesized by ALDH1A1, regulates synaptic scaling at glutamatergic synapses by regulating AMPAR trafficking [67]. Furthermore, ALDH1A1 is part of a highly conserved pathway that provides an alternative method of GABA-synthesis through putrescine [63]. Disrupting this pathway through decreasing ALDH1A1 might cause deprivation of backup pathways to synthesize GABA, which might in turn reduce inhibitory transmission, disrupting E/I tone. These findings support previous research, showing that male *fgf14*-/- mice exhibit changes in overall synaptic function as well as changes in response to drugs of abuse, such as cocaine and methamphetamine [31].

Changes in dopaminergic and GABAergic signaling in male *fgf14*-/- mice can also be attributed to decreased level of Protein Kinase A (PRKAR2B). PRKAR2B has been linked to GABA receptor breakdown by the endothelial gene Claudin-5 in the prefrontal cortex of patients with SZ [68], and may partially underlie the mechanism of action of several antipsychotics through the increase of GABA receptors [65,69]. PRKAR2B also plays a role in dopaminergic neuromodulation, though this has typically been shown in the nucleus accumbens for D2 receptor signaling as well as neuronal firing in medium spiny neurons [68,70–73]. Probes that target the interface between FGF14 and the voltage-gated Na+ channel 1.6 (Nav1.6) have been shown to disrupt medium spiny neuron firing, a phenotype that is found in the same neuron subtype in male *fgf14*-/- mice 14. It is plausible that PKA and FGF14 provide a regulatory mechanism of medium spiny neurons firing that contributes to maintain dopaminergic tone in the nucleus accumbens.

Other proteins with altered expression in the male *fgf14*-/- mice are members of pathways altered in neuropsychiatric disorders. Translin (Tsn) is an RNA binding protein that regulates the dendritic trafficking of brain derived neurotrophic factor (BDNF) [74]. BDNF is tied to synaptic transmission, plasticity and homeostasis and decreased serum level of BDNF and mutations in the BDNF receptor, Tyrosine Receptor Kinase B have been linked to SZ [75,76]. Though little is known about the effects of increased TSN [77], its altered expression in the male *fgf14*-/- mice, along with altered levels of expression of other key proteins, support the previous finding that the male *fgf14*-/- mouse model may be a new model of SZ and other disorders with disrupted cognition as a domain.

Overall, these findings support previous research that the *fgf14*-/- male animals have several key features that may constitute an endophenotype of SZ, especially cognitive symptoms of the disease [21]. As there are currently no pharmacotherapies for the treatment of the cognitive symptoms of SZ, this animal model may be a powerful tool in the discovery and testing of new disease treatments.

Of similar importance is the striking finding that the proteome of female *fgf14*-/- mice is drastically different from their male counterparts. This is especially critical given the gender differences in several domains of neuropsychiatric disorders, including age of diagnosis, premorbid functioning, and symptom clustering [37–41]. These results indicate that there is a need for more research into the potential behavioral changes, or lack thereof, of the female *fgf14*-/- mice compared to *fgf14*+/+ females. In fact, the upregulation of SNAP25 and MTATP6 not only indicate that female *fgf14*-/- mice have a unique proteomic signature, but may have a mechanism of resilience that compensates for changes in synaptic function seen in male mice at the same age.

SNAP25 is an important member of the SNAP/SNARE complex, which is necessary for the proper release of vesicles at the synapse [78] and has previously been shown to co-immunoprecipitate with FGF14 [10]. Not only is deletion of SNAP25 linked to an increase in E/I tone through increased glutamatergic neurotransmission [55], but deletion of SNAP25 has also been linked to improper neurogenesis in the adult mammalian brain, an important endophenotype of several neuropsychiatric disorders including SZ and bipolar disorder [79,80]. Previous research has shown that male *fgf14*-/- also show traits of an immature dentate gyrus [29]. These findings suggest that this could be mediated through SNAP25, though more research is needed to determine if neurogenesis is

also altered in the brain of adult female *fgf14-/-* mice. Decreases in both SNAP25 and MTATP6 have been seen in patients with SZ as well as potential animal models of neuropsychiatric disease [55,57,78,81,82]. Not only does our study highlight the importance of sex-specific research in basic science, it lays the groundwork for further investigations on the mechanisms of potential resilience to neuropsychiatric disorders in the females in preclinical models and human population.

Supplementary Materials: The following are available online at www.mdpi.com/xxx/s1, Figure S1: title, Table S1: Protein fold changes, Table S2: Autism and Schizophrenia associated genes, Table S3: Group-specific protein clusters

Author Contributions: Conceptualization, F.L., J.D., and M.S.; Validation, M.S.; Formal Analysis, M.S. and C.L.; Investigation, A.S.; Resources, F.L., K.Z., and C.L.; Data Curation, A.S.; Writing – Original Draft Preparation, J.D., M.S.; Writing – Review & Editing, F.L.; Visualization, P.W.; Supervision, F.L.; Project Administration, F.L. and K.Z.; Funding Acquisition, F.L. and K.Z.

Funding: This research was funded by NIH R01MH111107 (FL), R01MH095995 (FL), R01DA047102 (FL), R01CA184097 (KZ), NIA T32 AG051131 (PAW), and University of Texas Medical Branch Jeanne B. Kempner Scholarship (JD).

Conflicts of Interest: The authors declare no conflict of interest.

References

(1) Brusse, E.; de Koning, I.; Maat-Kievit, A.; Oostra, B. A.; Heutink, P.; van Swieten, J. C. Spinocerebellar Ataxia Associated with a Mutation in the Fibroblast Growth Factor 14 Gene (SCA27): A New Phenotype. Mov. Disord. 2006. https://doi.org/10.1002/mds.20708.

(2) Pablo, J. L.; Pitt, G. S. Fibroblast Growth Factor Homologous Factors. Neurosci. 2016, 22 (1), 19–25. https://doi.org/10.1177/1073858414562217.

(3) Groth, C. L.; Berman, B. D. Spinocerebellar Ataxia 27: A Review and Characterization of an Evolving Phenotype. Tremor Other Hyperkinet. Mov. (N. Y). 2018, 8, 534. https://doi.org/10.7916/D80S0ZJQ.

(4) Hoxha, E.; Tempia, F.; Lippiello, P.; Miniaci, M. C. Modulation, Plasticity and Pathophysiology of the Parallel Fiber-Purkinje Cell Synapse. Front. Synaptic Neurosci. 2016, 8, 35. https://doi.org/10.3389/fnsyn.2016.00035.

(5) Choquet, K.; La Piana, R.; Brais, B. A Novel Frameshift Mutation in FGF14 Causes an Autosomal Dominant Episodic Ataxia. Neurogenetics 2015, 16 (3), 233–236. https://doi.org/10.1007/s10048- 014-0436-7.

(6) Hoxha, E.; Balbo, I.; Miniaci, M. C.; Tempia, F. Purkinje Cell Signaling Deficits in Animal Models of Ataxia. Front. Synaptic Neurosci. 2018, 10, 6. https://doi.org/10.3389/fnsyn.2018.00006.

(7) Ornitz, D. M.; Itoh, N. The Fibroblast Growth Factor Signaling Pathway. Wiley Interdiscip. Rev. Dev. Biol. 4 (3), 215–266. https://doi.org/10.1002/wdev.176.

(8) Di Re, J.; Wadsworth, P. A.; Laezza, F. Intracellular Fibroblast Growth Factor 14 : Emerging Risk Factor for Brain Disorders. 2017, 11 (April), 1–7. https://doi.org/10.3389/fncel.2017.00103.

(9) Ali, S. R.; Singh, A. K.; Laezza, F. Identification of Amino Acid Residues in Fibroblast Growth Factor 14 (FGF14) Required for Structure-Function Interactions with Voltage-Gated Sodium Channel Nav1.6. J. Biol. Chem. 2016, 291 (21), 11268–11284. https://doi.org/10.1074/jbc.M115.703868.

(10) Bosch, M. K.; Nerbonne, J. M.; Townsend, R. R.; Miyazaki, H.; Nukina, N.; Ornitz, D. M.; Marionneau, C. Proteomic Analysis of Native Cerebellar IFGF14 Complexes. Channels 2016. https://doi.org/10.1080/19336950.2016.1153203.

(11) Hsu, W. C. J.; Scala, F.; Nenov, M. N.; Wildburger, N. C.; Elferink, H.; Singh, A. K.; Chesson, C. B.; Buzhdygan, T.; Sohail, M.; Shavkunov, A. S.; et al. CK2 Activity Is Required for the Interaction of FGF14 with Voltage-Gated Sodium Channels and Neuronal Excitability. FASEB J. 2016. https://doi.org/10.1096/fj.201500161.

(12) Laezza, F.; Gerber, B. R.; Lou, J.-Y.; Kozel, M. A.; Hartman, H.; Craig, A. M.; Ornitz, D. M.; Nerbonne, J. M. The FGF14(F145S) Mutation Disrupts the Interaction of FGF14 with Voltage- Gated Na+ Channels and Impairs Neuronal Excitability. J. Neurosci. 2007, 27 (44), 12033–12044. https://doi.org/10.1523/JNEUROSCI.2282-07.2007.

(13) Lou, J.-Y.; Laezza, F.; Gerber, B. R.; Xiao, M.; Yamada, K. A.; Hartmann, H.; Craig, A. M.; Nerbonne, J. M.; Ornitz, D. M. Fibroblast Growth Factor 14 Is an Intracellular Modulator of Voltage-Gated Sodium Channels. J Physiol 2005, 5691, 179–193. https://doi.org/10.1113/jphysiol.2005.097220.

(14) Ali, S. R.; Liu, Z.; Nenov, M. N.; Folorunso, O.; Singh, A. K.; Scala, F.; Chen, H.; James, T. F.; Alshammari, M.; Panova-Elektronova, N. I.; et al. Functional Modulation of Voltage-Gated Sodium Channels by a FGF14-Based Peptidomimetic. ACS Chem. Neurosci. 2018, acschemneuro.7b00399. https://doi.org/10.1021/acschemneuro.7b00399.

(15) Shavkunov, A. S.; Wildburger, N. C.; Nenov, M. N.; James, T. F.; Buzhdygan, T. P.; Panova-Elektronova, N. I.; Green, T. A.; Veselenak, R. L.; Bourne, N.; Laezza, F. The Fibroblast Growth Factor 14??Voltage-Gated Sodium Channel Complex Is a New Target of Glycogen Synthase Kinase 3 (GSK3). J. Biol. Chem. 2013, 288 (27), 19370–19385. https://doi.org/10.1074/jbc.M112.445924.

(16) Goldfarb, M.; Schoorlemmer, J.; Williams, A.; Diwakar, S.; Wang, Q.; Huang, X.; Giza, J.; Tchetchik, D.; Kelley, K.; Vega, A.; et al. Fibroblast Growth Factor Homologous Factors Control Neuronal Excitability through Modulation of Voltage-Gated Sodium Channels. Neuron 2007. https://doi.org/10.1016/j.neuron.2007.07.006.

(17) Goldfarb, M. Voltage-Gated Sodium Channel-Associated Proteins and Alternative Mechanisms of Inactivation and Block. Cellular and Molecular Life Sciences. 2012. https://doi.org/10.1007/s00018-011-0832-1.

(18) Tempia, F.; Hoxha, E.; Negro, G.; Alshammari, M. A.; Alshammari, T. K.; Panova-Elektronova, N.; Laezza, F. Parallel Fiber to Purkinje Cell Synaptic Impairment in a Mouse Model of Spinocerebellar Ataxia Type 27. Front. Cell. Neurosci. 2015, 9, 205. https://doi.org/10.3389/fncel.2015.00205.

(19) Yan, H.; Pablo, J. L.; Pitt, G. S. FGF14 Regulates Presynaptic Ca2+ Channels and Synaptic Transmission. Cell Rep. 2013. https://doi.org/10.1016/j.celrep.2013.06.012.

(20) Xiao, M.; Xu, L.; Laezza, F.; Yamada, K.; Feng, S.; Ornitz, D. M. Impaired Hippocampal Synaptic Transmission and Plasticity in Mice Lacking Fibroblast Growth Factor 14. Mol. Cell. Neurosci. 2007, 34 (3), 366–377. https://doi.org/10.1016/j.mcn.2006.11.020.

(21) Alshammari, T.; Alshammari, M.; Nenov, M.; Hoxha, E.; Cambiaghi, M.; Marcinno, A.; James, T.; Singh, P.; Labate, D.; Li, J.; et al. Genetic Deletion of Fibroblast Growth Factor 14 Recapitulates Phenotypic Alterations Underlying Cognitive Impairment Associated with Schizophrenia. Transl. Psychiatry 2016, 666. https://doi.org/10.1038/tp.2016.66.

(22) Hsu, W.-C.; Nenov, M. N.; Shavkunov, A.; Panova, N.; Zhan, M.; Laezza, F. Identifying a Kinase Network Regulating FGF14:Nav1.6 Complex Assembly Using Split-Luciferase Complementation. PLoS One 2015, 10 (2), e0117246. https://doi.org/10.1371/journal.pone.0117246.

(23) Hsu, W.-C. J.; Nilsson, C. L.; Laezza, F. Role of the Axonal Initial Segment in Psychiatric Disorders: Function, Dysfunction, and Intervention. Front. Psychiatry 2014, 5 (AUG), 109. https://doi.org/10.3389/fpsyt.2014.00109.

(24) Wildburger, N. C.; Laezza, F. Control of Neuronal Ion Channel Function by Glycogen Synthase Kinase-3: New Prospective for an Old Kinase. Front. Mol. Neurosci. 2012, 5, 80. https://doi.org/10.3389/fnmol.2012.00080.

(25) Scala, F.; Nenov, M. N.; Crofton, E. J.; Singh, A. K.; Folorunso, O.; Zhang, Y.; Chesson, B. C.; Wildburger, N. C.; James, T. F.; Alshammari, M. A.; et al. Environmental Enrichment and Social Isolation Mediate Neuroplasticity of Medium Spiny Neurons through the GSK3 Pathway. Cell Rep. 2018, 23 (2), 555–567. https://doi.org/10.1016/j.celrep.2018.03.062.

(26) Hoxha, E.; Marcinnò, A.; Montarolo, F.; Masante, L.; Balbo, I.; Ravera, F.; Laezza, F.; Tempia, F. Emerging Roles of Fgf14 in Behavioral Control. Behav. Brain Res. 2019, 356 (April 2018), 257–265. https://doi.org/10.1016/j.bbr.2018.08.034.

(27) Wozniak, D. F.; Xiao, M.; Xu, L.; Yamada, K. A.; Ornitz, D. M. Impaired Spatial Learning and Defective Theta Burst Induced LTP in Mice Lacking Fibroblast Growth Factor 14. Neurobiol. Dis. 2007. https://doi.org/10.1016/j.nbd.2006.11.014.

(28) Volk, L.; Chiu, S.-L.; Sharma, K.; Huganir, R. L. Glutamate Synapses in Human Cognitive Disorders. Annu. Rev. Neurosci. 2015, 38, 127–149. https://doi.org/10.1146/annurev-neuro-071714-033821.

(29) Alshammari, M. A.; Alshammari, T. K.; Nenov, M. N.; Scala, F.; Laezza, F. Fibroblast Growth Factor 14 Modulates the Neurogenesis of Granule Neurons in the Adult Dentate Gyrus. Mol. Neurobiol. 2016. https://doi.org/10.1007/s12035-015-9568-5.

(30) Sacco, R.; Cacci, E.; Novarino, G. Neural Stem Cells in Neuropsychiatric Disorders. Curr. Opin. Neurobiol. 2018, 48, 131–138. https://doi.org/10.1016/j.conb.2017.12.005.

(31) Wang, Q.; Bardgett, M. E.; Wong, M.; Wozniak, D. F.; Lou, J.; McNeil, B. D.; Chen, C.; Nardi, A.; Reid, D. C.; Yamada, K.; et al. Ataxia and Paroxysmal Dyskinesia in Mice Lacking Axonally Transported FGF14. Neuron 2002. https://doi.org/10.1016/S0896-6273(02)00744-4.

(32) Savanthrapadian, S.; Wolff, A. R.; Logan, B. J.; Eckert, M. J.; Bilkey, D. K.; Abraham, W. C. Enhanced Hippocampal Neuronal Excitability and LTP Persistence Associated with Reduced Behavioral Flexibility in the Maternal Immune Activation Model of Schizophrenia. Hippocampus 2013, 23 (12), 1395–1409. https://doi.org/10.1002/hipo.22193.

(33) Chen, C. M. A.; Stanford, A. D.; Mao, X.; Abi-Dargham, A.; Shungu, D. C.; Lisanby, S. H.; Schroeder, C. E.; Kegeles, L. S. GABA Level, Gamma Oscillation, and Working Memory Performance in Schizophrenia. NeuroImage Clin. 2014, 4, 531–539. https://doi.org/10.1016/j.nicl.2014.03.007.

(34) Kantrowitz, J. T.; Epstein, M. L.; Beggel, O.; Rohrig, S.; Lehrfeld, J. M.; Revheim, N.; Lehrfeld, N. P.; Reep, J.; Parker, E.; Silipo, G.; et al. Neurophysiological Mechanisms of Cortical Plasticity Impairments in Schizophrenia and Modulation by the NMDA Receptor Agonist D-Serine. Brain 2016, 139 (12), 3281–3295. https://doi.org/10.1093/brain/aww262.

(35) Falkenberg, L. E.; Westerhausen, R.; Craven, A. R.; Johnsen, E.; Kroken, R. A.; LØberg, E. M.; Specht, K.; Hugdahl, K. Impact of Glutamate Levels on Neuronal Response and Cognitive Abilities in Schizophrenia. NeuroImage Clin. 2014, 4, 576–584. https://doi.org/10.1016/j.nicl.2014.03.014.

(36) Frankle, W. G.; Cho, R. Y.; Prasad, K. M.; Mason, N. S.; Paris, J.; Himes, M. L.; Walker, C.; Lewis, D. A.; Narendran, R. In Vivo Measurement of GABA Transmission in Healthy Subjects and Schizophrenia Patients. Am. J. Psychiatry 2015, 172 (11), 1148–1159. https://doi.org/10.1176/appi.ajp.2015.14081031.

(37) McGlashan, T. H.; Bardenstein, K. K. Gender Differences in Affective, Schizoaffective, and Schizophrenic Disorders. Schizophr. Bull. 1990, 16 (2), 319–329.

(38) Morgan, V. A.; Castle, D. J.; Jablensky, A. V. Do Women Express and Experience Psychosis Differently from Men? Epidemiological Evidence from the Australian National Study of Low Prevalence (Psychotic) Disorders. Aust. N. Z. J. Psychiatry 2008, 42 (1), 74–82. https://doi.org/10.1080/00048670701732699.

(39) Shtasel, D. L.; Gur, R. E.; Gallacher, F.; Heimberg, C.; Gur, R. C. Gender Differences in the Clinical Expression of Schizophrenia. Schizophr. Res. 1992, 7 (3), 225–231.

(40) Ochoa, S.; Usall, J.; Cobo, J.; Labad, X.; Kulkarni, J. Gender Differences in Schizophrenia and First- Episode Psychosis: A Comprehensive Literature Review. Schizophr. Res. Treatment 2012, 2012, 1– 9. https://doi.org/10.1155/2012/916198.

(41) Pinares-Garcia, P.; Stratikopoulos, M.; Zagato, A.; Loke, H.; Lee, J. Sex: A Significant Risk Factor for Neurodevelopmental and Neurodegenerative Disorders. Brain Sci. 2018, 8 (8), 1–27. https://doi.org/10.3390/brainsci8080154.

(42) Mastro, R.; Hall, M. Protein Delipidation and Precipitation by Tri-n-Butylphosphate, Acetone, and Methanol Treatment for Isoelectric Focusing and Two-Dimensional Gel Electrophoresis. Anal. Biochem. 1999, 273 (2), 313–315. https://doi.org/10.1006/abio.1999.4224.

(43) Cox, J.; Mann, M. MaxQuant Enables High Peptide Identification Rates, Individualized p.p.b.-Range Mass Accuracies and Proteome-Wide Protein Quantification. Nat. Biotechnol. 2008, 26 (12), 1367–1372. https://doi.org/10.1038/nbt.1511.

(44) Tyanova, S.; Temu, T.; Cox, J. The MaxQuant Computational Platform for Mass Spectrometry-Based Shotgun Proteomics. Nat. Protoc. 2016, 11 (12), 2301–2319. https://doi.org/10.1038/nprot.2016.136.

(45) Tyanova, S.; Temu, T.; Sinitcyn, P.; Carlson, A.; Hein, M. Y.; Geiger, T.; Mann, M.; Cox, J. The Perseus Computational Platform for Comprehensive Analysis of (Prote)Omics Data. Nat. Methods 2016, 13 (9), 731–740. https://doi.org/10.1038/nmeth.3901.

(46) Papp, E. A.; Leergaard, T. B.; Calabrese, E.; Johnson, G. A.; Bjaalie, J. G. Waxholm Space Atlas of the Sprague Dawley Rat Brain. Neuroimage 2014, 97, 374–386. https://doi.org/10.1016/j.neuroimage.2014.04.001.

(47) Sergejeva, M.; Papp, E. A.; Bakker, R.; Gaudnek, M. A.; Okamura-Oho, Y.; Boline, J.; Bjaalie, J. G.; Hess, A. Anatomical Landmarks for Registration of Experimental Image Data to Volumetric Rodent Brain Atlasing Templates. J. Neurosci. Methods 2015, 240, 161–169. https://doi.org/10.1016/j.jneumeth.2014.11.005.

(48) Kjonigsen, L. J.; Lillehaug, S.; Bjaalie, J. G.; Witter, M. P.; Leergaard, T. B. Waxholm Space Atlas of the Rat Brain Hippocampal Region: Three-Dimensional Delineations Based on Magnetic Resonance and Diffusion Tensor Imaging. Neuroimage 2015, 108, 441–449. https://doi.org/10.1016/j.neuroimage.2014.12.080.

(49) Bähner, F.; Meyer-Lindenberg, A. Hippocampal–prefrontal Connectivity as a Translational Phenotype for Schizophrenia. Eur. Neuropsychopharmacol. 2017, 27 (2), 93–106. https://doi.org/10.1016/j.euroneuro.2016.12.007.

(50) Chevaleyre, V.; Piskorowski, R. A. Hippocampal Area CA2: An Overlooked but PromisingTherapeutic Target. Trends Mol. Med. 2016, 22 (8), 645–655. https://doi.org/10.1016/j.molmed.2016.06.007.

(51) Kang, E.; Wen, Z.; Song, H.; Christian, K. M.; Ming, G. Adult Neurogenesis and Psychiatric Disorders. Cold Spring Harb. Perspect. Biol. 2016, 8 (9), a019026. https://doi.org/10.1101/cshperspect.a019026.

(52) Nakahara, S.; Adachi, M.; Ito, H.; Matsumoto, M.; Tajinda, K.; Erp, T. G. M. van. Hippocampal Pathophysiology: Commonality Shared by Temporal Lobe Epilepsy and Psychiatric Disorders. Neurosci. J. 2018, 2018, 1–9. https://doi.org/10.1155/2018/4852359.

(53) Bielow, C.; Mastrobuoni, G.; Kempa, S. Proteomics Quality Control: Quality Control Software for MaxQuant Results. J. Proteome Res. 2016, 15 (3), 777–787. https://doi.org/10.1021/acs.jproteome.5b00780.

(54) Gu, Y.; Chiu, S.-L.; Liu, B.; Wu, P.-H.; Delannoy, M.; Lin, D.-T.; Wirtz, D.; Huganir, R. L. Differential Vesicular Sorting of AMPA and GABA A Receptors. Proc. Natl. Acad. Sci. 2016, 113 (7), E922– E931. https://doi.org/10.1073/pnas.1525726113.

(55) Yang, H.; Zhang, M.; Shi, J.; Zhou, Y.; Wan, Z.; Wang, Y.; Wan, Y.; Li, J.; Wang, Z.; Fei, J. Brain-Specific SNAP-25 Deletion Leads to Elevated Extracellular Glutamate Level and Schizophrenia-Like Behavior in Mice. Neural Plast. 2017, 2017. https://doi.org/10.1155/2017/4526417.

(56) Hjelm, B. E.; Rollins, B.; Mamdani, F.; Lauterborn, J. C.; Kirov, G.; Lynch, G.; Gall, C. M.; Sequeira, A.; Vawter, M. P. Evidence of Mitochondrial Dysfunction within the Complex Genetic Etiology of Schizophrenia. Mol. Neuropsychiatry 2015, 1 (4), 201–219. https://doi.org/10.1159/000441252.

(57) Ueno, H.; Nishigaki, Y.; Kong, Q.-P.; Fuku, N.; Kojima, S.; Iwata, N.; Ozaki, N.; Tanaka, M. Analysis of Mitochondrial DNA Variants in Japanese Patients with Schizophrenia. Mitochondrion 2009, 9 (6), 385–393. https://doi.org/10.1016/j.mito.2009.06.003.

(58) Brisch, R.; Bielau, H.; Saniotis, A.; Wolf, R.; Bogerts, B.; Krell, D.; Steiner, J.; Braun, K.; Krzyżanowska, M.; Krzyżanowski, M.; et al. Calretinin and Parvalbumin in Schizophrenia and Affective Disorders: A Mini-Review, a Perspective on the Evolutionary Role of Calretinin in Schizophrenia, and a Preliminary Post-Mortem Study of Calretinin in the Septal Nuclei. Front. Cell. Neurosci. 2015, 9, 393. https://doi.org/10.3389/fncel.2015.00393.

(59) Peretti, D.; Bastide, A.; Radford, H.; Verity, N.; Molloy, C.; Martin, M. G.; Moreno, J. A.; Steinert, J. R.; Smith, T.; Dinsdale, D.; et al. RBM3 Mediates Structural Plasticity and Protective Effects of Cooling in Neurodegeneration. Nature 2015, 518 (7538), 236–239. https://doi.org/10.1038/nature14142.

(60) Seyfried, N. T.; Dammer, E. B.; Swarup, V.; Nandakumar, D.; Duong, D. M.; Yin, L.; Deng, Q.; Nguyen, T.; Hales, C. M.; Wingo, T.; et al. A Multi-Network Approach Identifies Protein-Specific Co-Expression in Asymptomatic and Symptomatic Alzheimer's Disease. Cell Syst. 2017, 4 (1), 60–72.e4. https://doi.org/10.1016/j.cels.2016.11.006.

(61) de Leeuw, C. A.; Mooij, J. M.; Heskes, T.; Posthuma, D. MAGMA: Generalized Gene-Set Analysis of GWAS Data. PLoS Comput. Biol. 2015, 11 (4), e1004219. https://doi.org/10.1371/journal.pcbi.1004219.

(62) Zhou, G.; Xia, J. OmicsNet: A Web-Based Tool for Creation and Visual Analysis of Biological Networks in 3D Space. Nucleic Acids Res. 2018, 46 (W1), W514–W522. https://doi.org/10.1093/nar/gky510.

(63) Kim, J.-I.; Ganesan, S.; Luo, S. X.; Wu, Y.-W.; Park, E.; Huang, E. J.; Chen, L.; Ding, J. B. Aldehyde Dehydrogenase 1a1 Mediates a GABA Synthesis Pathway in Midbrain Dopaminergic Neurons. Science (80-.). 2015, 350 (6256), 102–106. https://doi.org/10.1126/science.aac4690.

(64) Liu, G.; Yu, J.; Ding, J.; Xie, C.; Sun, L.; Rudenko, I.; Zheng, W.; Sastry, N.; Luo, J.; Rudow, G.; et al. Aldehyde Dehydrogenase 1 Defines and Protects a Nigrostriatal Dopaminergic Neuron Subpopulation. J. Clin. Invest. 2014, 124 (7), 3032–3046. https://doi.org/10.1172/JCI72176.

(65) Adams, M. R.; Brandon, E. P.; Chartoff, E. H.; Idzerda, R. L.; Dorsa, D. M.; McKnight, G. S. Loss of Haloperidol Induced Gene Expression and Catalepsy in Protein Kinase A-Deficient Mice. Proc. Natl. Acad. Sci. 1997, 94 (22), 12157–12161. https://doi.org/10.1073/pnas.94.22.12157.

(66) Chang, S.; Fang, K.; Zhang, K.; Wang, J. Network-Based Analysis of Schizophrenia Genome-Wide Association Data to Detect the Joint Functional Association Signals. PLoS One 2015, 10 (7), e0133404. https://doi.org/10.1371/journal.pone.0133404.

(67) Aoto, J.; Nam, C. I.; Poon, M. M.; Ting, P.; Chen, L. Synaptic Signaling by All-Trans Retinoic Acid in Homeostatic Synaptic Plasticity. Neuron 2008, 60 (2), 308–320. https://doi.org/10.1016/j.neuron.2008.08.012.

(68) Nishiura, K.; Ichikawa-Tomikawa, N.; Sugimoto, K.; Kunii, Y.; Kashiwagi, K.; Tanaka, M.; Yokoyama, Y.; Hino, M.; Sugino, T.; Yabe, H.; et al. PKA Activation and Endothelial Claudin-5 Breakdown in the Schizophrenic Prefrontal Cortex. Oncotarget 2017, 8 (55), 93382–93391. https://doi.org/10.18632/oncotarget.21850.

(69) Pan, B.; Lian, J.; Huang, X.-F.; Deng, C. Aripiprazole Increases the PKA Signalling and Expression of the GABAA Receptor and CREB1 in the Nucleus Accumbens of Rats. J. Mol. Neurosci. 2016, 59 (1), 36–47. https://doi.org/10.1007/s12031-016-0730-y.

(70) Chen, Y.; Yu, F. H.; Surmeier, D. J.; Scheuer, T.; Catterall, W. A. Neuromodulation of Na+ Channel Slow Inactivation via CAMP-Dependent Protein Kinase and Protein Kinase C. Neuron 2006, 49 (3), 409–420. https://doi.org/10.1016/j.neuron.2006.01.009.

(71) Maurice, N.; Tkatch, T.; Meisler, M.; Sprunger, L. K.; Surmeier, D. J. D1/D5 Dopamine Receptor Activation Differentially Modulates Rapidly Inactivating and Persistent Sodium Currents in Prefrontal Cortex Pyramidal Neurons. J. Neurosci. 2001, 21 (7), 2268–2277.

(72) Flores-Hernandez, J.; Hernandez, S.; Snyder, G. L.; Yan, Z.; Fienberg, A. A.; Moss, S. J.; Greengard, P.; Surmeier, D. J. D(1) Dopamine Receptor Activation Reduces GABA(A) Receptor Currents in Neostriatal Neurons through a PKA/DARPP-32/PP1 Signaling Cascade. J. Neurophysiol. 2000, 83 (5), 2996–3004. https://doi.org/10.1152/jn.2000.83.5.2996.

(73) Surmeier, D. J.; Bargas, J.; Hemmings, H. C.; Nairn, A. C.; Greengard, P. Modulation of Calcium Currents by a D1 Dopaminergic Protein Kinase/Phosphatase Cascade in Rat Neostriatal Neurons. Neuron 1995, 14 (2), 385–397.

(74) Wu, Y.-C.; Williamson, R.; Li, Z.; Vicario, A.; Xu, J.; Kasai, M.; Chern, Y.; Tongiorgi, E.; Baraban, J.M. Dendritic Trafficking of Brain-Derived Neurotrophic Factor MRNA: Regulation by Translin- Dependent and -Independent Mechanisms. J. Neurochem. 2011, 116 (6), 1112–1121. https://doi.org/10.1111/j.1471-4159.2010.07166.x.

(75) Libman-Sokołowska, M.; Drozdowicz, E.; Nasierowski, T. BDNF as a Biomarker in the Course and Treatment of Schizophrenia. Psychiatr. Pol. 2015, 49 (6), 1149–1158. https://doi.org/10.12740/PP/37705.

(76) Kheirollahi, M.; Kazemi, E.; Ashouri, S. Brain-Derived Neurotrophic Factor Gene Val66Met Polymorphism and Risk of Schizophrenia: A Meta-Analysis of Case-Control Studies. Cell. Mol. Neurobiol. 2016, 36 (1), 1–10. https://doi.org/10.1007/s10571-015-0229-z.

(77) Ishida, R.; Okado, H.; Sato, H.; Shionoiri, C.; Aoki, K.; Kasai, M. A Role for the Octameric Ring Protein, Translin, in Mitotic Cell Division. FEBS Lett. 2002, 525 (1–3), 105–110.

(78) Antonucci, F.; Corradini, I.; Fossati, G.; Tomasoni, R.; Menna, E.; Matteoli, M. SNAP-25, a Known Presynaptic Protein with Emerging Postsynaptic Functions. Front. Synaptic Neurosci. 2016, 8. https://doi.org/10.3389/fnsyn.2016.00007.

(79) Hagihara, H.; Takao, K.; Walton, N. M.; Matsumoto, M.; Miyakawa, T. Immature Dentate Gyrus: An Endophenotype of Neuropsychiatric Disorders. Neural Plast. 2013, 2013, 318596. https://doi.org/10.1155/2013/318596.

(80) Yamasaki, N.; Maekawa, M.; Kobayashi, K.; Kajii, Y.; Maeda, J.; Soma, M.; Takao, K.; Tanda, K.; Ohira, K.; Toyama, K.; et al. Alpha-CaMKII Deficiency Causes Immature Dentate Gyrus, a Novel Candidate Endophenotype of Psychiatric Disorders. Mol. Brain 2008, 1, 6. https://doi.org/10.1186/1756-6606-1-6.

(81) Thompson, P. M.; Egbufoama, S.; Vawter, M. P. SNAP-25 Reduction in the Hippocampus of Patients with Schizophrenia. Prog. Neuro-Psychopharmacology Biol. Psychiatry 2003, 27 (3), 411–417. https://doi.org/10.1016/S0278-5846(03)00027-7.

(82) Etain, B.; Dumaine, A.; Mathieu, F.; Chevalier, F.; Henry, C.; Kahn, J. P.; Deshommes, J.; Bellivier, F.; Leboyer, M.; Jamain, S. A SNAP25 Promoter Variant Is Associated with Early-Onset Bipolar Disorder and a High Expression Level in Brain. Mol. Psychiatry 2010, 15 (7), 748–755. https://doi.org/10.1038/mp.2008.148.